Computers and Structures xxx (2011) xxx–xxx

Contents lists available at ScienceDirect

Computers and Structures

journal homepage: www.elsevier.com/locate/compstruc

A new method of fictitious viscous damping determination for the dynamic relaxation method

M. Rezaiee-pajand [a], M. Kadkhodayan [b,*], J. Alamatian [c], L.C. Zhang [d]

[a] Department of Civil Engineering, The Ferdowsi University of Mashhad, Mashhad, Iran
[b] Department of Mechanical Engineering, The Ferdowsi University of Mashhad, Mashhad, Iran
[c] Department of Civil Engineering, The Islamic Azad University, Mashhad Branch, Mashhad, Iran
[d] School of Mechanical and Manufacturing Engineering, The University of New South Wales NSW 2052, Australia

ARTICLE INFO

Article history:
Received 25 June 2009
Accepted 1 February 2011
Available online xxxx

Keywords:
Dynamic relaxation
Fictitious viscous damping
Lowest eigenvalue
Nonlinear analysis

ABSTRACT

This paper develops a new method for calculating the viscous fictitious damping of the dynamic relaxation (DR) method to overcome one of the most crucial difficulties in its application – the low convergence rate. The DR formulation was derived by error minimizations between two successive iterations to deduce an optimum fictitious mass and viscous damping with the aid of the Stodola iterative process. The efficiency of the new method was verified by its application to a wide range of typical structures with strong nonlinearity. The results show that compared to the conventional DR algorithm such as kinetic approach, the new method improves the convergence rate considerably.

1. Introduction

A structural analysis often needs the solution to a set of equations,

$$[S]\{D\} = \{f\} = \{P\} \tag{1}$$

using a numerical method, such as the finite element method or the finite difference method, where $[S]$ is the structural stiffness matrix, and $\{D\}$, $\{f\}$ and $\{P\}$ are displacement, internal force and external load vectors, respectively. When a geometrical, material or contact nonlinearity in involved, the internal force vector will be a nonlinear function of the displacement. The most commonly used methods for solving Eq. (1) in nonlinear analysis are iterative techniques, either implicit or explicit [1]. An explicit method uses residual force so that calculations can be performed by a vector operation which is simple and highly efficient for nonlinear problems. An implicit method, on the other hand, is formulated based on residual force derivatives (stiffness matrix) and requires a matrix operation, which make them more complex and time consuming. For example, at a snap-through or a snap-back point of a structure, when the stiffness matrix becomes zero or undefined, the implicit method will encounter difficulties although its convergence rate is generally greater than that of the explicit.

The dynamic relaxation (DR) method [2,3] is an explicit iterative technique which converts a static system to an artificially dynamic one by adding fictitious inertia and damping forces. When the artificial dynamic motion diminishes, i.e., when the system returns to its static state, a solution to the original static problem is obtained. In so doing, Eq. (1) becomes

$$[M]^n\{\ddot{D}\}^n + [C]^n\{\dot{D}\}^n + [S]^n\{D\}^n = \{f\}^n = \{P\}^n, \tag{2}$$

where $[M]^n$ and $[C]^n$ are fictitious mass and damping matrices in the nth iteration of the DR algorithm, respectively, which are always diagonal for the sake of simplicity. The super dots denote the derivatives related to the fictitious time. Mathematically, the DR formulation is based on the second order Richardson rule [4]. Physically, DR scheme can be illustrated by the steady state response of an artificially dynamic system [5,6].

Rushton [7] applied DR to nonlinear systems. Brew and Brotton formulated the DR method using the first order dynamic equilibrium relationship and studied the stability conditions of frame structures [8]. Wood defined fictitious mass using the upper bound of spectral radius of the coefficient matrix [9] and showed that by doing so the convergence rate of DR became higher than the semi-iterative procedures in linear analysis. Bunce [10] conducted an estimation of critical damping. Alwar et al. determined the steady state response from an exponential function [11]. Cassell and Hobbs utilized Gerschgörin circle theory for fictitious mass values and applied this method for nonlinear problems [12]. Also kinetic damping theory was proposed by Cundall [13].

Frieze et al. [14] used a DR algorithm for nonlinear analysis of plates. Papadrakakis [15] carried out an error analysis and suggested an automatic procedure for the selection of DR parameters.

* Corresponding author.
E-mail address: kadkhoda@um.ac.ir (M. Kadkhodayan).

0045-7949/$ - see front matter © 2011 Elsevier Ltd. All rights reserved.
doi:10.1016/j.compstruc.2011.02.002

Another explicit formulation was performed by Underwood [16]. An implicit DR relationship was introduced by Felippa [17]. Zienkiewicz and Lohner suggested an accelerated procedure for improvement of the convergence rate [18]. Barnes used DR method for form-finding of prestressed nets and membranes structures [19]. By using weighting factors for mass and damping, Al-Shawi and Mardirosian utilized DR in the finite element analysis of plate bending [20]. Qiang determined fictitious time and damping by Rayleigh's principle [21]. A modified adaptive DR method, the maDR algorithm, was proposed by Zhang and Yu in which the estimation of steady state response was modified to be instant [22].

Other researchers such as Turvey et al. [23] and Bardet et al. [24] studied some applications of DR method. Ramesh and Krishnamoorthy [25,26] applied the DR method to problems with snap-through or snap-back. Kadkhodayan et al. [27–29] introduced a new model for fictitious damping and analyzed elastic-plastic plate bending and buckling. Also, Topping et al used Parallel Dynamic Relaxation technique for finite element analysis [30,31]. Nonlinear analysis of buckling propagation in pipe lines [32], shape finding [33,34] and grid shells, spline beams and membrane analysis [35,36] are other applications of the DR method. In addition, the DR has been combined with neural networks to increase model accuracy of tensegrity structures [37] and has been successfully applied to linear and nonlinear analysis of composite structures [38]. Moreover, Topping and Ivanyi in a recent book have concentrated on the computational aspects of analysis and design of cable membrane structures using the dynamic relaxation method with a finite element idealization [39]. This book provides a comprehensive view to the DR procedure and its parameters for structural finite element analysis. Modifications of fictitious time steps have been formulated based on the minimization of residual forces in DR iterations [40]. Recently, the method has also been used in nonlinear dynamic analysis of structures [41].

In the explicit DR method, fundamental relationships are constructed by using the central finite difference formulation as follows [22]:

$$\dot{D}_i^{n+\frac{1}{2}} = \frac{2m_{ii} - t^n c_{ii}}{2m_{ii} + t^n c_{ii}} \dot{D}_i^{n-\frac{1}{2}} + \frac{2t^n}{2m_{ii} + t^n c_{ii}} r_i^n \qquad i = 1, 2, \ldots, q, \tag{3}$$

$$D_i^{n+1} = D_i^n + t^{n+1} \dot{D}_i^{n+\frac{1}{2}} \qquad i = 1, 2, \ldots, q, \tag{4}$$

where t^n, m_{ii} and c_{ii} are fictitious time step, ith diagonal element of fictitious mass and damping matrices in the nth iteration of DR, respectively. Notation q denotes the number of degrees of freedom and r_i^n is the residual force of the ith degree of freedom, i.e., $\{R\}^n$ in the nth iteration:

$$\{R\}^n = [M]^n \{\ddot{D}\}^n + [C]^n \{\dot{D}\}^n = \{P\}^n - \{f\}^n. \tag{5}$$

DR iterations are unstable because numerical time integration is used to integrate the differential equations of motion. Hence, fictitious parameters such as time step and diagonal mass and damping matrices are determined so that the stability conditions are satisfied. However, the slow convergence rate of the DR method has always been a critical issue.

This paper will introduce a new approach to determine the fictitious damping in the dynamic relaxation method based on the Stodola iterative process together with an instant adaptive criterion. It should be emphasized that two general types of damping can be utilized in DR process: *Kinetic damping* and *Viscous damping*.

Many parameters have to be set in order to obtain an efficient solution for any structural problem. However, the number of parameters may be reduced by using kinetic damping which does not require the determination of a viscous damping term, so that only the time step and the fictitious nodal masses are required. In this way, the time interval may be fixed [39]. Hence, the kinetic damping provides an alternative approach for DR method. This procedure has been proposed by Cundall [13] for application to unstable rock mechanism. The high stability and rapid convergence rate for structures with large displacement are the main specification of the kinetic damping method. In such analyses, the undamped motion of a structure is traced until local peak in total kinetic energy is detected. Then all current velocities are reset to zero and DR process is restarted with current geometry and repeated through further peaks (generally decreasing) until the energy of all modes of vibration have been dissipated (static equilibrium) [30]. The method of kinetic damping has been found to be very stable and rapidly convergent when dealing with large displacements [39]. The stability of this method depends on the time–mass relation [36]. One of the important applications of kinetic damping DR algorithm is parallel finite element analysis [30,31,39]. For example, the Dynamic Relaxation method can be used based upon geometric parallelism [30]. The parallel DR scheme is undertaken in two stages. First, the overall mesh is divided into different number of sub domains corresponding to the number of available processors. Then, DR process (usually DR with kinetic damping algorithm) is used over the sub domains and converged results from each sub domain are received and compiled to obtain the overall results for the domain.

On the other hand, the viscous damping which has been used in several common DR algorithms such as Papadrakakis [15], Underwood [16], and etc., is closer to real dynamic exercise. The DR formulation which is described in this paper is based on viscous damping.

This paper focuses on viscous damping and presents a new approach to calculate this factor so that DR convergence rate of proposed technique is higher than the common existing methods. The merits of the new method will be verified by a comparison with the nonlinear finite element solutions to some typical structures. Moreover, the proposed viscous DR method will be compared with the common kinetic DR algorithm.

2. Error analysis of the viscous dynamic relaxation method

In this section, the viscous damping for DR method is considered. The most common way to study the stability and convergence rate of a viscous DR algorithm is an error analysis between two successive iterations. Substituting Eq. (3) into Eq. (4) and using the previous velocity $\left(\dot{D}_i^{n-\frac{1}{2}}\right)$ as a function of displacement leads to the following relationship:

$$\left(2 + \frac{t^n c_{ii}}{m_{ii}}\right) D_i^{n+1} = \left(2 + \frac{t^n c_{ii}}{m_{ii}}\right) D_i^n + \frac{t^{n+1}}{t^n} \left(2 - \frac{t^n c_{ii}}{m_{ii}}\right) (D_i^n - D_i^{n-1}) + \frac{2t^{n+1} t^n}{m_{ii}} (p_i - f_i^n) \qquad i = 1, 2, \ldots, q \tag{6}$$

The differential form of the fundamental DR equation, Eq. (6), is as follows:

$$\left(2 + \frac{t^n c_{ii}}{m_{ii}}\right) dD_i^{n+1} = \left(2 + \frac{t^n c_{ii}}{m_{ii}}\right) dD_i^n + \frac{t^{n+1}}{t^n} \left(2 - \frac{t^n c_{ii}}{m_{ii}}\right) (dD_i^n - dD_i^{n-1}) + \frac{2t^{n+1} t^n}{m_{ii}} dr_i^n \qquad i = 1, 2, \ldots, q \tag{7}$$

where dD_i^n is the increment of displacement of the ith degree of freedom in the nth DR iteration. If the external load is assumed to be constant during successive iterations, i.e., when $dp_i = 0$, the increment of the residual force, dr_i^n, can be formulated based on the chain derivative rule:

$$dr_i^n = -df_i^n = -\sum_{j=1}^{q} \frac{\partial f_i^n}{\partial D_j^n} dD_j^n = -\sum_{j=1}^{q} s_{ij}^n dD_j^n, \tag{8}$$

Please cite this article in press as: Rezaiee-pajand M et al. A new method of fictitious viscous damping determination for the dynamic relaxation method. Comput Struct (2011), doi:10.1016/j.compstruc.2011.02.002

The tangent stiffness matrix ([S]) can be calculated analytically or numerically. The error factor k_i ($i = 1, 2, \ldots, q$) is defined as

$$dD_i^{n+1} = k_i dD_i^n, \quad dD_i^{n-1} = \frac{1}{k_i} dD_i^n \quad i = 1,2,\ldots,q. \tag{9}$$

If the fictitious time step is assumed to be constant between two iterations ($t^n = t^{n+1}$), substituting Eq. (9) into Eq. (7) gives

$$\left(2 + \frac{t^n c_{ii}}{m_{ii}}\right) k_i^2 - 2[2 - (t^n)^2 \lambda_i] k_i + 2 - \frac{t^n c_{ii}}{m_{ii}} = 0 \qquad i = 1,2,\ldots,q, \tag{10}$$

where λ_i is the ith eigenvalue of matrix $[M]^{-1}$ [s] defined by the following eigenvalue problem:

$$[M]^{-1}[S]\{dD\} - \lambda[I]\{dD\} = \{0\} \rightarrow [S]\{dD\} - \lambda[M]\{dD\} = \{0\}, \tag{11}$$

where $[I]$ is a unit matrix. It is clear that λ_i is the square of the natural frequency of the artificial dynamic system constructed by the following equation:

$$|[S] - \lambda[M]| = 0. \tag{12}$$

On the other hand, the error factor can be calculated from Eq. (10), i.e.,

$$k_i = \frac{2 - (t^n)^2 \lambda_i \pm \sqrt{\Delta_i'}}{2 + t^n c_{ii}/m_{ii}} \qquad i = 1,2,\ldots,q. \tag{13}$$

where

$$\Delta_i' = (t^n c_{ii}/m_{ii})^2 + (t^n)^4 \lambda_i^2 - 4(t^n)^2 \lambda_i \quad i = 1,2,\ldots,q. \tag{14}$$

The DR stability and convergence rate conditions are satisfied if the error factor, which is a function of two quantities, $\frac{t^n c_{ii}}{m_{ii}}$ and λ_i, is minimized. Fig. 1a shows the variation of the error factor for $\lambda = 1.0$. It is clear that the error factor is minimized when Eq. (10) has two equal roots for k_i. Fig. 1b demonstrates that it is also true for other eigenvalues. Therefore, the necessary condition for the maximum convergence rate is obtained when the discriminant of Eq. (10) (Δ_i') is equal to zero;

$$\Delta_i' = 0 \rightarrow (t^n c_{ii}/m_{ii})^2 + (t^n)^4 \lambda_i^2 - 4(t^n)^2 \lambda_i = 0 \qquad i = 1,2,\ldots,q. \tag{15}$$

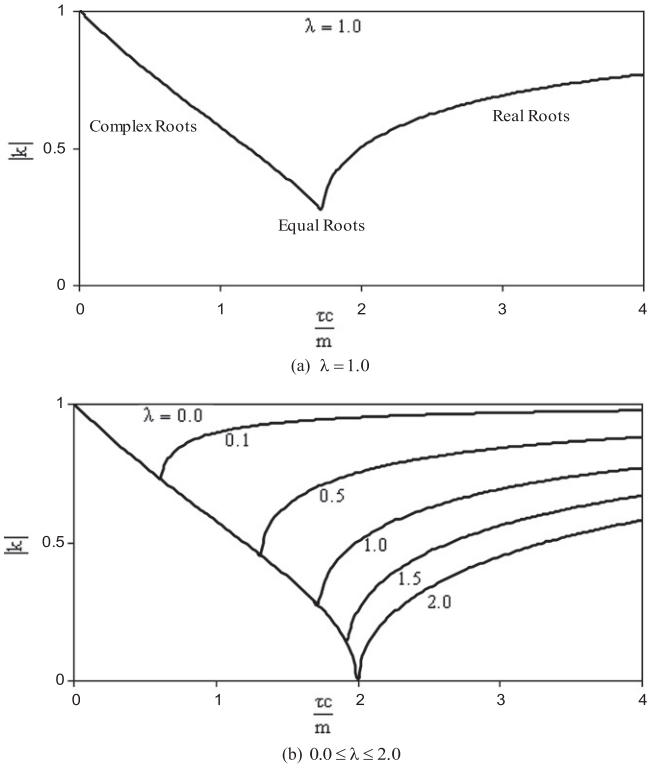

(a) $\lambda = 1.0$

(b) $0.0 \le \lambda \le 2.0$

Fig. 1. Variation of the error factor.

Fig. 1b shows the acceptable domains for fictitious parameters (mass, damping and time step). In order to guarantee the maximum stability, it is necessary that the absolute value of the error factor is less than unity. Hence, $\frac{t^n c_{ii}}{m_{ii}}$ should be selected in the following domain:

$$0 < \frac{t^n c_{ii}}{m_{ii}} \leqslant 2. \tag{16}$$

On the other hand, Eq. (15), which is an important condition for calculating DR parameters, can be transformed to a second order equation as

$$(t^n)^4 \lambda_i^2 - 4(t^n)^2 \lambda_i + (t^n c_{ii}/m_{ii})^2 = 0 \qquad i = 1,2,\ldots,q. \tag{17}$$

Therefore, the upper and lower bounds of the ith eigenvalue are obtained as

$$\lambda_i^U = \frac{2 + \sqrt{4 - (t^n c_{ii}/m_{ii})^2}}{(t^n)^2} \qquad i = 1,2,\ldots,q. \tag{18}$$

$$\lambda_i^L = \frac{2 - \sqrt{4 - (t^n c_{ii}/m_{ii})^2}}{(t^n)^2} \qquad i = 1,2,\ldots,q. \tag{19}$$

Then, the acceptable domain for the upper and lower bounds of each eigenvalue can be calculated by the combination of Eq. (16) with Eqs. (18) and (19), i.e.,

$$\frac{2}{(t^n)^2} \leqslant \lambda_i^U < \frac{4}{(t^n)^2} \qquad i = 1,2,\ldots,q. \tag{20}$$

$$0 < \lambda_i^L \leqslant \frac{2}{(t^n)^2} \qquad i = 1,2,\ldots,q. \tag{21}$$

Moreover, the eigenvalues of matrix $[M]^{-1}$ can be estimated by the Gerschgörin's circle theory as [42]

$$\left|\lambda_i - \frac{s_{ii}}{m_{ii}}\right| \leqslant \frac{1}{m_{ii}} \sum_{\substack{j=1 \\ j \neq i}}^{q} |S_{ij}| \qquad i = 1,2,\ldots,q, \tag{22}$$

Hence, each eigenvalue can be laid in two discrete regions, (I) and (II), which are obtained by the sign determination of Eq. (22), i.e.,

$$\lambda_i \in \mathrm{I} \Rightarrow \frac{1}{m_{ii}} s_{ii} \leqslant \lambda_i \leqslant \frac{1}{m_{ii}} \sum_{j=1}^{q} |s_{ij}| \quad i = 1,2,\ldots,q. \tag{23}$$

$$\lambda_i \in \mathrm{II} \Rightarrow \frac{1}{m_{ii}} \left[s_{ii} - \sum_{\substack{j=1 \\ j \neq i}}^{q} |s_{ij}| \right] \leqslant \lambda_i \leqslant \frac{1}{m_{ii}} s_{ii} \qquad i = 1,2,\ldots,q. \tag{24}$$

Although both the zones are correct, it can be proved that Zone (I) is more suitable for structural analysis (see Appendix). Because the boundary identified by Zone (I) (Eq. (21)) should satisfy Conditions (20) and (21), the following relationships can be obtained:

$$\frac{2}{(t^n)^2} \leqslant \lambda_i^U < \frac{4}{(t^n)^2} \rightarrow \frac{(t^n)^2}{4} \sum_{j=1}^{q} |s_{ij}| < m_{ii} \leqslant \frac{(t^n)^2}{2} \sum_{j=1}^{q} |s_{ij}| \qquad i = 1,2,\ldots,q, \tag{25}$$

$$0 < \lambda_i^L \leqslant \frac{2}{(t^n)^2} \rightarrow \frac{(t^n)^2}{2} s_{ii} \leqslant m_{ii} < \infty \qquad i = 1,2,\ldots,q. \tag{26}$$

One of the important criteria to assess the DR convergence is the residual force, the sum of the inertia and damping forces. By choos-

Please cite this article in press as: Rezaiee-pajand M et al. A new method of fictitious viscous damping determination for the dynamic relaxation method. Comput Struct (2011), doi:10.1016/j.compstruc.2011.02.002

ing the minimum acceptable value for fictitious mass, inertia force and consequently the residual force reduction, the lower boundary of the mass region (in Eqs. (25) and (26)) is selected for the fictitious mass:

$$m_{ii} = \frac{(t^n)^2}{4} \max\left[2s_{ii}, \sum_{j=1}^{q} |s_{ij}|\right] \qquad i = 1, 2, \ldots, q \tag{27}$$

To start the viscous DR iterations, the fictitious damping should be determined. The damping factor that causes the structure to approach the static position most rapidly should be used for the analysis. This factor is called the critical damping factor. The critical damping factor may be estimated by undertaking an undamped run to obtain an estimate of the highest frequency and by using the expression derived for the critical damping factor for a one degree of freedom problem. The undamped trail analysis is sometimes referred to as the "trail run" [39]. Unlike the commonly used fictitious damping calculation method [27], i.e.,

$$c_{ii} = 2m_{ii}\omega_{\min} = 2m_{ii}\sqrt{\lambda_{\min}} \qquad i = 1, 2, \ldots, q, \tag{28}$$

where $\omega_{\min}$ is the lowest natural frequency of a structure in free vibration, in our present formulation, the fictitious damping can be determined by Eq. (15), leading to

$$c_{ii} = m_{ii}\sqrt{4\lambda_i - (t^n)^2\lambda_i^2} \qquad i = 1, 2, \ldots, q. \tag{29}$$

Based on the structural dynamics theory, the effect of higher deformation modes is much less than the lower ones. In other words, one can neglect the higher frequencies without a considerable error but with a much enhanced computation efficiency. Hence, the lowest natural frequency can be used for damping calculations in Eq. (29), which gives rise to

$$c_{ii} = m_{ii}\sqrt{4\lambda_{\min} - (t^n)^2\lambda_{\min}^2} \qquad i = 1, 2, \ldots, q. \tag{30}$$

When the lowest natural frequency approaches zero, Eq. (30) reduces to Eq. (28). Hence, the commonly used method of fictitious damping determination is a special, approximate case of our new method.

3. The lowest natural frequency by Stodola method

An important point that still remains up to this point is to find an accurate and simple technique to calculate the lowest natural frequency, because this has a great effect on the viscous DR convergence rate. The majority of the previous investigations used the Rayleigh principle, which, when applied to a structure as a whole, the lowest natural frequency is determined by [27]

$$\omega_{\min}^2 = \lambda_{\min} \approx \frac{(\{D\}^n)^T\{f\}^n}{(\{D\}^n)^T[M]^n\{D\}^n}. \tag{31}$$

If it is applied to a single joint, the lowest natural frequency can be calculated on each node, separately, as [29]

$$(\omega_{\min}^i)^2 = \lambda_{\min}^i \approx \frac{(\{D^i\}^n)^T\{f^i\}^n}{(\{D^i\}^n)^T[M^i]^n\{D^i\}^n} \qquad i = 1, 2, \ldots, h, \tag{32}$$

where ω_{min}^i, $\{D^i\}^n$, $\{f^i\}^n$ and $[M^i]^n$ are the lowest frequency, displacement, internal force vector and fictitious mass matrices of the ith node, respectively, and h indicates the total number of nodes of the structure. Another way is to apply the Rayleigh principle to each degree of freedom. In this case, the ith eigenvalue of $[M]^{-1}$ can be calculated as

$$\omega_i^2 = \lambda_i \approx \frac{f_i}{m_{ii}D_i} \qquad i = 1, 2, \ldots, q. \tag{33}$$

However, all methods based on the Rayleigh principle are approximate so that their accuracy is a concern. In the following, we propose a new method for calculating the lowest natural frequency for DR iterations.

The Stodola iterative process can be used in the DR algorithm. The steps to calculate the lowest natural frequency using the Stodola iterative process are as follow [43,44]:

(a) Assume initial eigenvector for the lowest natural frequency ($\{\overline{X}^0\} = \{I\}$) and set $i = 0$.
(b) Determine $\{X^{i+1}\}$ by

$$\{X^{i+1}\} = [S_T]^{-1}[M]\{\overline{X}^i\}. \tag{34}$$

(c) Normalize the eigenvector with respect to the largest elements of this vector, i.e.,

$$\{\overline{X}^{i+1}\} = \frac{\{X^{i+1}\}}{\max(X^{i+1})}. \tag{35}$$

(d) Check the convergence by comparing two successive eigenvectors,

$$\frac{|(\{\overline{X}^{i+1}\})^T\{\overline{X}^{i+1}\} - (\{\overline{X}^i\})^T\{\overline{X}^i\}|}{(\{\overline{X}^{i+1}\})^T\{\overline{X}^{i+1}\}} \leqslant \text{tolerance}. \tag{36}$$

(e) If the convergence criterion is not satisfied go back to (b); otherwise obtain the lowest eigenvalue from the following equation:

$$\lambda_{\min} = \max(X^{i+1}). \tag{37}$$

The above Stodola iterative process requires the inverse of the stiffness matrix in each of the DR iterations. For a smooth nonlinear analysis, the lowest frequency can be considered a constant at each load increment in DR iterations – a constant lowest frequency (CLF) method – hence the calculation of the inverse stiffness matrix is not a significant concern. If a structure is strongly nonlinear, the lowest frequency should be updated frequently, which will reduce the computational efficiency drastically. Here we propose an approach to automatically update the lowest frequency to realize a rapid convergence rate.

To achieve this, it is necessary to introduce a criterion for updating the lowest frequency when required. The variation of the residual force between successive iterations is a good quantity to use. If the residual force does not vary considerably or remains constant during three iterations, the DR convergence rate has become slow, indicating that the lowest natural frequency should be updated. In other words, when the absolute difference of the residual force ratio between three successive iterations ($n-2$, $n-1$ and n) approaches zero (or less than a small allowable value e_n), i.e.,

$$\left|\frac{\sqrt{\sum_{i=1}^{q}(r_i^n)^2}}{\sqrt{\sum_{i=1}^{q}(r_i^{n-1})^2}} - \frac{\sqrt{\sum_{i=1}^{q}(r_i^{n-1})^2}}{\sqrt{\sum_{i=1}^{q}(r_i^{n-2})^2}}\right| < e_n, \tag{38}$$

the convergence rate is slow. At this stage the lowest natural frequency should be updated at the nth iteration. For convenience, we call it an updated lowest frequency (ULF) method.

Using our ULF above, we can construct various viscous DR algorithms, i.e., CDF, WRP, NRP and DRP as defined in Table 1, using different damping theories. In this paper, we will calculate the mass matrix by Eq. (27). The fictitious time step is constant and equal to unity for all algorithms. In the CDF and WRP algorithms, the lowest natural frequency of a structure as a whole is calculated from the Rayleigh principle, i.e., Eq. (31).

Please cite this article in press as: Rezaiee-pajand M et al. A new method of fictitious viscous damping determination for the dynamic relaxation method. Comput Struct (2011), doi:10.1016/j.compstruc.2011.02.002

Table 1
The damping specifications of viscous dynamic relaxation algorithms.

Algorithm name	Description	Damping relation	Eigenvalue calculations
CDF	Common damping factor	Eq. (28)	Rayleigh principle, Eq. (31)
WRP	Rayleigh principle for whole system	Eq. (30)	Rayleigh principle, Eq. (31)
NRP	Rayleigh principle for each node	Eq. (30)	Rayleigh principle, Eq. (32)
DRP	Rayleigh principle for each degree of freedom	Eq. (30)	Rayleigh principle, Eq. (33)
CLF	Constant lowest frequency	Eq. (30)	Stodola process in first iteration
ULF	Updated lowest frequency	Eq. (30)	Stodola process when condition (38) is satisfied

4. The kinetic DR algorithm

The kinetic DR method proposed by Cundall [13] is an efficient procedure to reduce the DR parameters. This algorithm does not require the calculation of fictitious viscous damping, i.e., this procedure traces the undamped vibrations of structure to obtain the static equilibrium position. Therefore, the fundamental iterative relationships of kinetic DR method can be achieved when the viscous damping factor in Eqs. (3) and (4), is equal to zero ($c_{ii} = 0$), i.e.;

$$\dot{D}_i^{n+\frac{1}{2}} = \dot{D}_i^{n-\frac{1}{2}} + \frac{t^n}{m_{ii}} r_i^n \qquad i = 1, 2, \ldots, q, \tag{39}$$

$$D_i^{n+1} = D_i^n + t^{n+1} \dot{D}_i^{n+\frac{1}{2}} \qquad i = 1, 2, \ldots, q, \tag{40}$$

By running Eqs. (39) and (40) successively, the total kinetic energy of undamped structure is traced during iterations. A position with maximum kinetic energy would represent the static equilibrium where the potential energy is a minimum. The kinetic DR algorithm uses this idea to approach the static equilibrium position. In each iteration, the total kinetic energy, U_k, is calculated by the following equation:

$$U_k = \sum_{i=1}^{q} m_{ii} \left(\dot{D}_i^{n+\frac{1}{2}} \right)^2 \tag{41}$$

DR iterations run successively, until a peak in the kinetic energy is detected. At this stage, all current velocities are reset to zero. This process should be continued through further peaks until the convergence criterions are satisfied. To apply this algorithm, it is assumed that the peak of kinetic energy has occurred between times t^n and t^{n+1}, i.e., a fall in the total kinetic energy has taken place at time t^{n+1}. As described by Topping and Ivanyi [39], the displacement of the peak of kinetic energy is calculated by the following equation:

$${}^{*}D_i^n = D_i^{n+1} - \frac{3}{2} t^{n+1} \dot{D}_i^{n+\frac{1}{2}} + \frac{(t^n)^2}{2 m_{ii}} r_i^n \qquad i = 1, 2, \ldots, q, \tag{42}$$

where, ${}^{*}D_i^n \quad i = 1, 2, \ldots, q$ is the displacement with maximized kinetic energy. The analysis is restarted by taking the ${}^{*}D_i^n \quad i = 1, 2, \ldots, q$ as the initial displacements. To obtain a better convergence, the velocities of the first time step should be calculated at the mid point as bellow:

$$\dot{D}_i^{n+\frac{1}{2}} = \frac{t^n}{2 m_{ii}} r_i^n \qquad i = 1, 2, \ldots, q, \tag{43}$$

where, r_i^n is calculated from displacement's components, presented by Eq. (42). Now, the DR iterations are restarted from Eqs. (39) and (40). The above process will be continued for other successive peaks of kinetic energy until the convergence criteria are satisfied. This algorithm is called KDR.

The diagonal elements of mass matrix which control the stability of kinetic DR algorithm (KDR), have been formulated as follows [39]:

$$m_{ii} \geqslant \frac{(t^n)^2}{2} \sum_{j=1}^{q} |s_{ij}| \qquad i = 1, 2, \ldots, q \tag{44}$$

5. Numerical examples and discussion

The DR algorithms presented in Sections 3 and 4 dealing with viscous and kinetic approaches, respectively, are utilized to analyze some structures. Here two criterions are employed for better judgment about the efficiency of different DR schemes i.e., *number of convergence DR iterations* and *variation of the structural displacement during convergence DR iterations*. By the first criterion the convergence rate of algorithms are compared. The second criterion shows that which model has more efficiency for structural analysis. Moreover, a comparison between the viscous and kinetic DR methods can be performed.

To investigate the capability of our new algorithms, CLF and ULF, some typical elastic structures with geometrical nonlinearity are analyzed by the finite element method. For this purpose, some programs have been written by the authors in Fortran Power Station software. The results' validity and accuracy of these programs have been checked and controlled by several benchmark problems which have been achieved from the published papers. Wide range of such numerical examples proved the accuracy and validity of the proposed programs. Because of paper limitation, we cannot present all numerical results. Here, some of the important ones are considered. The truss-spring system to be discussed is a nonlinear single degree of freedom system with both softening and hardening behaviors. This kind of structure has been used as a benchmark problem for examining the efficiency and capacity of an algorithm. The toggle and portal frames are skeletal structures with two types of degrees of freedom (transformation and rotation). They have high softening nonlinearity and can be used to verify the capability of the proposed methods for strongly nonlinear structures. The space truss has many degrees of freedom and can be used to examine the capability of the proposed methods for large structures with high degrees of freedom. The circular plate, spherical cap and cone shell are continuous structures with hardening and/or softening behavior. In all the calculations, e_n in Criterion (38) is taken as 0.005.

5.1. Truss spring system

The truss-spring system illustrated in Fig. 2 is a nonlinear one degree of freedom structure, composed of a spring of stiffness

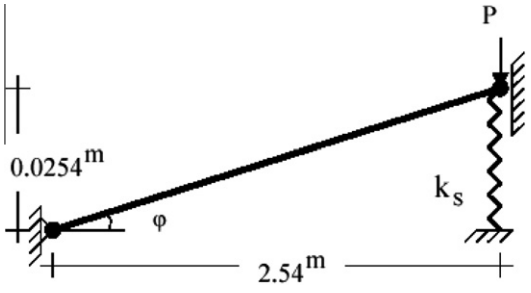

Fig. 2. A truss-spring system.

Please cite this article in press as: Rezaiee-pajand M et al. A new method of fictitious viscous damping determination for the dynamic relaxation method. Comput Struct (2011), doi:10.1016/j.compstruc.2011.02.002

K_S = 1051 N/m and a truss element of axial rigidity AE = 44 484 kN. This element is made of steel with modulus of elasticity and cross sectional area as 2.06×10^{11} N/m^2 and 2.16×10^{-4} m^2, respectively. According to Ref. [16], its internal force, f, and tangent stiffness, S_T, can be described by

$$f(D) = 0.5\mathrm{AE}(\cos^2\varphi)\left(\frac{D}{L_0}\right)^2\left[\frac{D}{L_0}\cos^2\varphi - 3\sin\varphi\right] + k_s D + \left(\mathrm{AE}\frac{D}{L_0}\right)\sin^2\varphi, \quad (45)$$

$$S_T = 1.5\mathrm{AE}(\cos^2\varphi)\left[\frac{D}{L_0}\cos^2\varphi - 2\sin\varphi\right]\left(\frac{D}{L_0^2}\right) + k_s + \frac{\mathrm{AE}\sin^2\varphi}{L_0}. \quad (46)$$

In our calculation, the loading process was completed in twelve increments with a constant load increment of 4.4484 N. Fig. 3 shows the load-deflection curve of this system. The number of iterations for convergence shows that the proposed algorithms, CLF or ULF, bring about a reduction of iterations of up to 60.7% and 75.4% compared to the CDF and WRP, respectively (Table 2). In this example, the kinetic DR method (KDR) does not show a good efficiency and its number of iterations for convergence is more than that of DR algorithms using viscous damping. Fig. 4 demonstrates the variation of displacement vs. convergence iterations at the 6th load increment when the nonlinearity of the structure emerges. It is clear that in this case the damping factor from the CLF is close to the critical damping such that a convergence to the steady state response is quickly reached.

5.2. Toggle frame

Fig. 5 shows a two-member frame with fixed supports that has been investigated both experimentally and analytically [45]. This structure is made of wood with modulus of elasticity as 0.71×10^{11} N/m^2. The total load (P), cross-sectional area and moment area of frame members are 155.605 N, 1.181×10^{-4} m^2, and 0.0375×10^{-8} m^4, respectively. In the present study, this structure was analyzed by five elements in each member. The

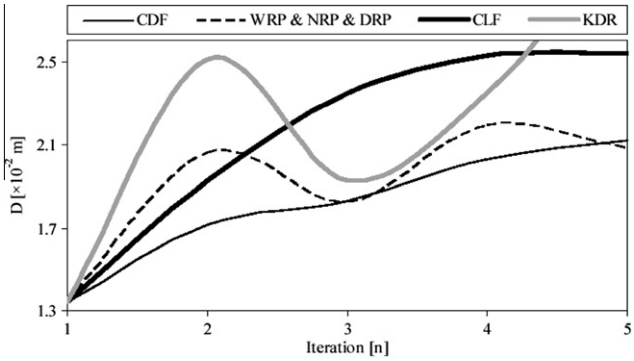

Fig. 4. Variation of displacement of the truss-spring system during the 6th load increment.

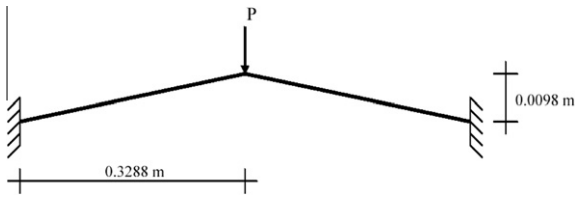

Fig. 5. A toggle frame.

co-rotational finite element formulation [1] was used and the total load was applied in ten equal increments. Fig. 6 displays the static path of the vertical deflection of the upper node. The number of iterations for convergence is listed in Table 3. In this example, the convergence rate of KDR algorithm (kinetic DR) is higher than viscous DR methods. However, the proposed ULF method could overcome this defect somehow so that its total iterations (5236) are close to the number of KDR's iterations (5069). In the ULF method, the lowest frequency was updated about every eleven iterations, leading to the highest convergence rate (in category of viscous DR method) of a maximum reduction of iterations of up

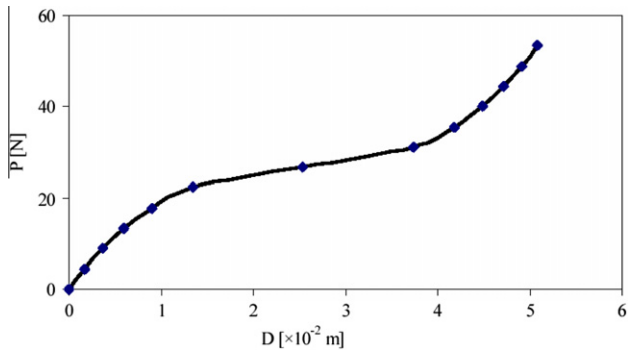

Fig. 3. The load-deflection curve of the truss-spring system.

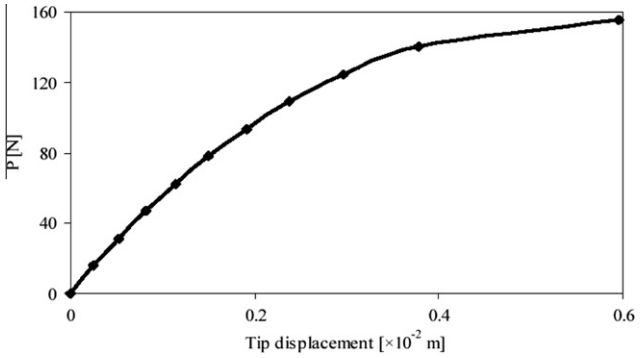

Fig. 6. The load-deflection curve of the toggle frame.

Table 2
The number of iterations for convergence in analyzing the truss-spring system.

Method	Number of iterations for each load increment												Total	Improvement (%)	
	1	2	3	4	5	6	7	8	9	10	11	12		$\frac{CDF-CLF}{CDF}$	$\frac{WRP-CLF}{WRP}$
CDF	17	17	19	21	26	45	17	11	6	8	9	11	207	60.7	75.4
WRP	5	6	8	11	19	61	7	9	11	12	13	13	175		
CLF & ULF	3(1)	3(1)	3(1)	3(1)	4(1)	4(1)	6(1)	4(1)	4(1)	3(1)	3(1)	3(1)	43(10)		
KDR	21	26	26	31	36	18	36	41	31	31	26	26	349		

Please cite this article in press as: Rezaiee-pajand M et al. A new method of fictitious viscous damping determination for the dynamic relaxation method. Comput Struct (2011), doi:10.1016/j.compstruc.2011.02.002

Table 3
The number of iterations for convergence in analyzing the toggle frame.

Method	Number of iterations for each load increment										Total	Improvement(%)	
	1	2	3	4	5	6	7	8	9	10		$\frac{DRP-ULF}{DRP}$	$\frac{CLF-ULF}{CLF}$
CDF	500	500	500	500	500	500	500	500	532	3781	8313	24.9	28.1
WRP	500	500	500	500	500	500	500	500	532	3780	8312		
NRP	500	500	500	500	500	500	500	500	500	2510	7010		
DRP	500	500	500	500	500	500	500	500	500	2473	6973		
CLF	500(1)	500(1)	500(1)	500(1)	500(1)	500(1)	500(1)	500(1)	500(1)	2785(1)	7285(10)		
ULF	500(57)	500(38)	500(44)	500(71)	500(36)	500(62)	500(32)	500(30)	500(76)	736(29)	5236(475)		
KDR	500	500	500	500	500	500	500	500	500	569	5069		

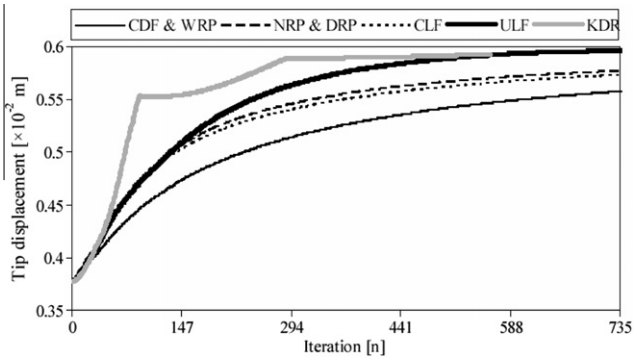

Fig. 7. Variation of the tip displacement of the toggle frame during the 10th load increment.

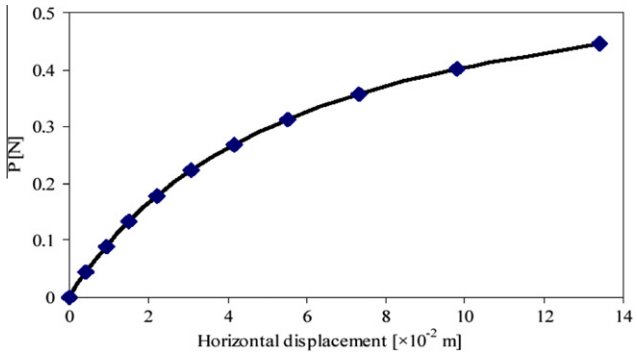

Fig. 9. The load-horizontal displacement curve of the portal frame.

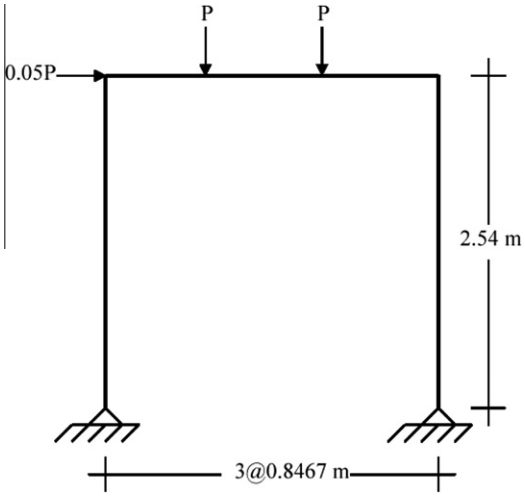

Fig. 8. A portal frame.

to 24.9% compared to the DRP. It is clear that calculating the lowest eigenvalue in the first iteration without further updating is not efficient, when a structure has intense nonlinearity. The ULF and KDR methods converge to the steady state at a semi-critical damping model, see Fig. 7, while the CDF, WRP, NRP and DRP experience over damped processes.

5.3. Portal frame

Each of the three members of the portal frame in Fig. 8 was modeled by three frame elements [1]. This structure is made of rubbery material with modulus of elasticity as 8274037.9 N/m^2. Also, the cross-section area and moment area of elements were taken as 12.9032×10^{-4} m^2 and 27.74876171×10^{-8} m^4, respectively. The total load P of 0.44484 N was applied in ten equal increments. Fig. 9 illustrates the load-deflection path of the horizontal displacement at the top of the frame. The number of iterations for convergence is shown in Table 4, which demonstrates that the lowest frequency had been automatically updated in about every eighty-four iterations by the algorithm Criterion (38). In this example, the KDR algorithm has a wonderful efficiency compared with viscous DR methods, so that the number of iteration is approximately third of that for the ULF one.

In the viscous DR algorithms, the convergence rate of the DRP, CLF and ULF are similar, but those of the CDF, WRP and NRP are

Table 4
The number of iterations for convergence in analyzing the portal frame.

Method	Number of iterations for each load increment										Total	Improvement (%)	
	1	2	3	4	5	6	7	8	9	10		$\frac{WRP-ULF}{WRP}$	$\frac{CLF-ULF}{CLF}$
CDF	500	13,740	8295	8441	8941	9653	10,559	11,687	13,105	14,946	99,867	76.2	7.4
WRP	500	13,733	8294	8440	8941	9653	10,559	11,687	13,105	14,946	99,858		
NRP	500	11,199	6602	6775	7123	7613	8278	9036	10,028	11,269	78,423		
DRP	2592	2189	1977	1931	2353	2008	2027	2341	2737	3312	23,467		
CLF	1686(1)	1747(1)	1882(1)	2027(1)	2220(1)	2433(1)	2712(1)	3081(1)	3571(1)	4261(1)	25,620(10)		
ULF	1686(13)	1746(12)	1811(10)	1953(17)	2107(28)	2314(28)	2585(31)	2771(41)	3169(43)	3573(57)	23,715(280)		
KDR	720	755	782	810	834	901	937	962	1071	1210	8982		

Please cite this article in press as: Rezaiee-pajand M et al. A new method of fictitious viscous damping determination for the dynamic relaxation method. Comput Struct (2011), doi:10.1016/j.compstruc.2011.02.002

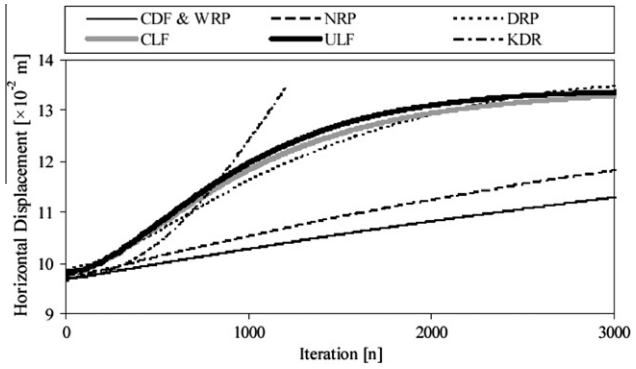

Fig. 10. Variation of the horizontal displacement of the portal frame during the 10th load increment.

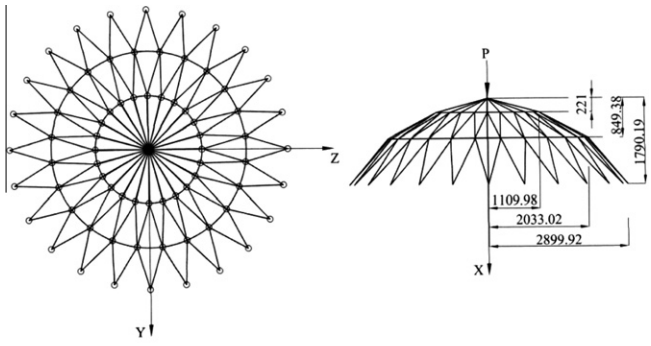

Fig. 11. A space truss.

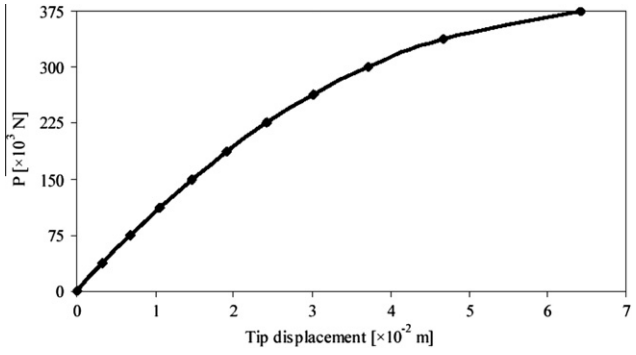

Fig. 12. The load-deflection curve at the tip of the space truss.

very low. Again and in the category of viscous DR methods, the ULF is the fastest, leading to a maximum reduction of iterations of up to 76.2% compared to the WRP. Fig. 10 shows that the ULF, CLF and

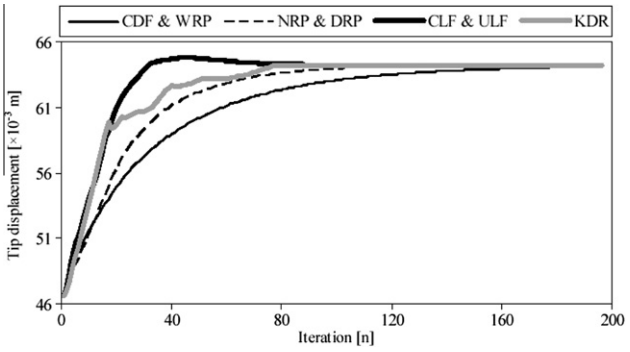

Fig. 13. Variation of the tip displacement of the space truss during the 10th load increment.

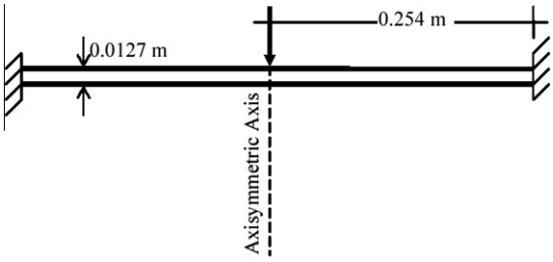

Fig. 14. A circular plate under a central concentrated load.

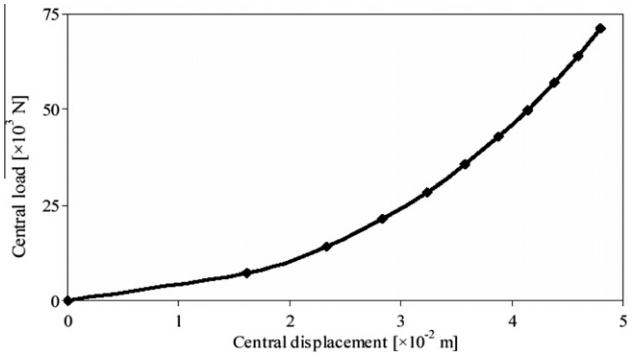

Fig. 15. The load-deflection curve of the circular plate.

DRP methods converge to the steady state response at the critical damping model, while the CDF, WRP, NRP undergo over damped processes. In this figure, the KDR algorithm has the quickest convergence rate.

5.4. Space truss

Fig. 11 illustrates a space truss which has been constructed from steel with modulus of elasticity 2.06×10^{11} N/m^2. The area

Table 5
The number of iterations for convergence in analyzing the space truss.

Method	Number of iterations for each load increment										Total	Improvement (%)	
	1	2	3	4	5	6	7	8	9	10		$\frac{WRP-ULF}{WRP}$	$\frac{DRP-ULF}{DRP}$
CDF	237	231	231	232	233	235	238	244	264	562	2707	31.8	95.9
WRP	235	229	229	230	231	234	237	243	263	559	2690		
NRP	2795	4901	6472	6799	7126	8560	7964	8574	10738	11,817	75,746		
DRP	2387	2908	2835	3876	4023	4508	5736	6121	5585	7577	45,556		
CLF	179(1)	180(1)	180(1)	180(1)	180(1)	182(1)	187(1)	183(1)	183(1)	198(1)	1832(1)		
ULF	179(1)	180(1)	180(3)	180(2)	180(4)	182(5)	187(3)	183(1)	183(4)	198(3)	1832(27)		
KDR	161	170	152	169	168	163	166	162	175	243	1729		

Please cite this article in press as: Rezaiee-pajand M et al. A new method of fictitious viscous damping determination for the dynamic relaxation method. Comput Struct (2011), doi:10.1016/j.compstruc.2011.02.002

Table 6
The number of iterations for convergence in analyzing the circular plate.

Method	Number of iterations for each load increment										Total	Improvement (%)	
	1	2	3	4	5	6	7	8	9	10		$\frac{WRP-ULF}{WRP}$	$\frac{CLF-ULF}{CLF}$
CDF	955	830	776	738	709	685	664	646	631	617	7251	52.3	8.7
WRP	955	830	775	737	708	684	663	646	630	616	7244		
NRP	712	779	777	828	852	818	782	814	739	772	7873		
DRP	764	762	947	861	860	827	800	817	809	790	8237		
CLF	758(1)	491(1)	402(1)	361(1)	338(1)	311(1)	294(1)	287(1)	271(1)	269(1)	3782(10)		
ULF	530(7)	429(4)	379(5)	338(3)	326(7)	307(8)	292(2)	289(5)	285(8)	275(11)	3452(60)		
KDR	677	530	487	493	520	503	297	331	418	434	4690		

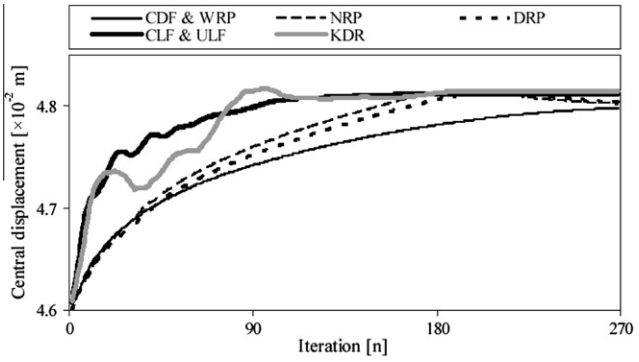

Fig. 16. Variation of the central displacement of the circular plate during the 10th load increment.

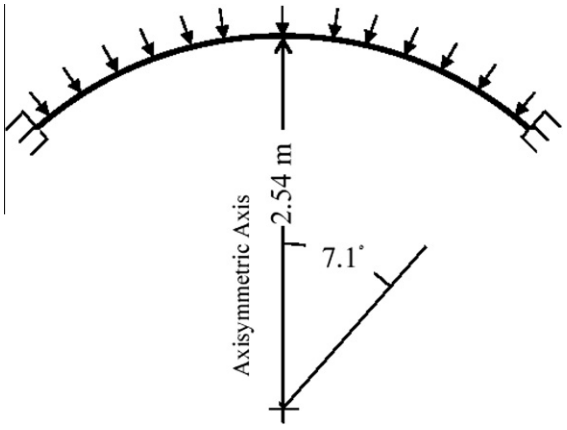

Fig. 17. A spherical cap under a uniformly distributed load.

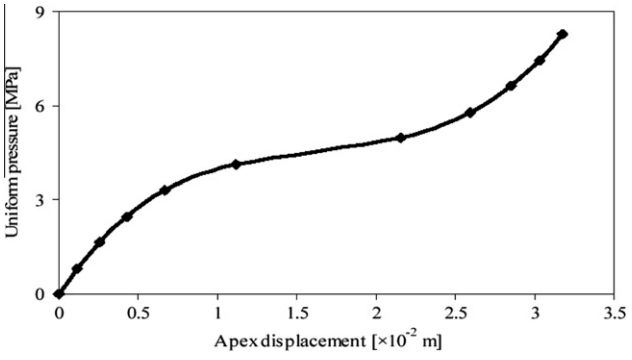

Fig. 18. The load-deflection curve of the spherical cap.

section of each member is 2.16×10^{-4} m^2. All support conditions are pined. This structure has 73 nodes, 168 elements and 147 degrees of freedom [46]. The total external load is 375 kN and the nodes in altitude $Z = 0$ are restrained in all directions. An elastic geometrical nonlinear analysis with Lagrangian finite element formulation was performed for ten loading increments [1]. Fig. 12 shows the load-deflection curves of the tip node in Z-direction. The number of iterations for convergence is listed in Table 5. Although the convergence rate of KDR algorithm is higher than that of the viscous DR methods; the proposed ULF and CLF methods could overcome this defect so that the difference between the convergence rates of KDR and ULF (or CLF) algorithms is approximately 5%. It should be noted that the convergence rate of KDR method is lower than that of the ULF (or CLF) in 10th load increment when there is an intense nonlinearity.

On the other hand, using the proposed method increases the efficiency of viscous DR algorithm, so that the proposed CLF and ULF methods converge faster than those using the Rayleigh principle. For example, the ULF method achieves a maximum reduction up to 31.8% and 95.9% compared with the WRP and DRP, respectively. Criterion (38) makes the lowest frequency updating happen in about every sixty-seven iterations in the ULF method. Fig. 13 shows that the KDR, ULF and CLF methods converge to the steady state response at a close-to-critical damping model, whereas the CDF, WRP, NRP and DRP take over damped processes.

5.5. Circular plate

A clamped circular plate under a concentrated central load was analyzed using five axisymmetric shell elements with geometrical nonlinear behavior [47], Fig. 14. The material is steel with modulus of elasticity 2.06×10^{11} N/m^2 and Poisson's ratio = 0.3. The total concentrated load of 71.168 kN was applied in ten equal increments. The central vertical displacement vs. load is plotted in Fig. 15. The number of required iterations for the convergence in the algorithms is listed in Table 6. In this example, the efficiency of the proposed viscous DR methods (ULF and CLF) is higher than that of the kinetic DR scheme (KDR). Using ULF and CLF, a considerable reduction about 25% and 20% has been occurred in the number of convergence iterations compared with the KDR, respectively.

Here, the ULF algorithm has the maximum convergence rate, giving rise to a maximum reduction up to 52.3% and 8.7% compared to the WRP and CLF methods, respectively. Clearly, Criterion (38) is adequate in promoting the DR convergence rate. The calculation of the ULF method shows that the lowest frequency should be updated in every fifty-seven iterations (Table 6). At the intense nonlinearity of the structure as shown by the variation of the central displacement vs. iterations at the 10th load increment in Fig. 16, the ULF and CLF methods converge to the steady state with close-to-critical damping, whereas all the other methods using the Rayleigh principle experience over damping. Moreover, the KDR

Please cite this article in press as: Rezaiee-pajand M et al. A new method of fictitious viscous damping determination for the dynamic relaxation method. Comput Struct (2011), doi:10.1016/j.compstruc.2011.02.002

Table 7
The number of iterations for convergence in analyzing the spherical cap.

Method	Number of iterations for each load increment										Total	Improvement (%)	
	1	2	3	4	5	6	7	8	9	10		$\frac{NRP-ULF}{NRP}$	$\frac{CLF-ULF}{CLF}$
CDF	440	477	533	633	930	1146	659	546	488	448	6300	10.1	22.0
WRP	439	477	532	633	930	1146	659	545	487	448	6296		
NRP	334	407	467	568	758	1513	682	478	450	379	6036		
DRP	389	413	415	509	929	1693	725	574	421	388	6456		
CLF	463(1)	501(1)	597(1)	800(1)	1590(1)	988(1)	704(1)	483(1)	439(1)	395(1)	6960(10)		
ULF	455(2)	410(41)	467(68)	558(73)	844(244)	865(58)	550(5)	494(2)	388(7)	392(10)	5423(510)		
KDR	448	349	330	468	633	652	492	437	412	335	4556		

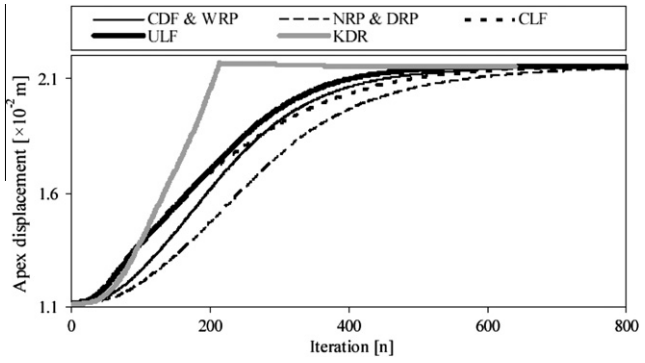

Fig. 19. Variation of the apex displacement of the spherical cap during the 6th load increment.

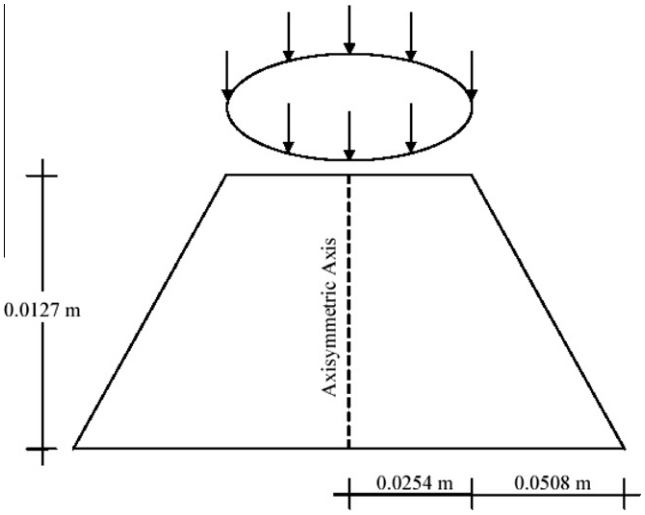

Fig. 20. A cone shell under an end circular ring load.

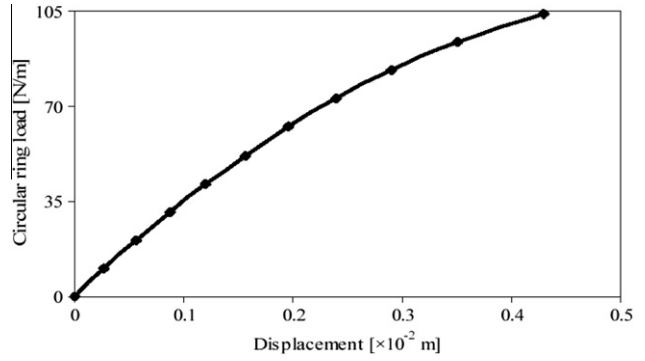

Fig. 21. Variation of the tip displacement of the cone shell during the 10th load increment.

method has some fluctuates when it converges to the static equilibrium.

5.6. Spherical cap

Fig. 17 shows a clamped spherical cap under a uniformly distributed load [47]. The thickness of the axisymmetric shell is 1.27 cm. This structure has been constructed from steel with modulus of elasticity and Poisson's ratio as 2.06×10^{11} N/m^2 and 0.3, respectively. Three axisymmetric shell elements with geometrical nonlinear behavior were used in our analysis. Similarly, the loading process was completed in ten equal increments to the total load of 8277300 N/m^2. Fig. 18 demonstrates the apex load vs. displacement, and Table 7 lists the number of required iterations for convergence. In this example, the convergence rate of KDR algorithm is higher than that of the viscous DR methods. However, the proposed ULF method could reduce this defect so that the difference between the convergence rates of KDR and ULF algorithms is about 15%.

On the other hand, using the proposed method increases the efficiency of viscous DR algorithm. The proposed ULF algorithm has the maximum convergence rate, which results in a maximum reduction of up to 11.2% and 23.0% compared to the NRP and CLF, respectively, when the lowest frequency in the ULF method is updated once every ten iterations in average. Fig. 19 shows the variations of the displacement vs. iterations at the 6th load increment when the structure has a more intense nonlinear behavior. Although the KDR has the most rapidly convergence rate to the static equilibrium, the ULF method approaches to the steady state with a close-to-critical damping.

5.7. Cone shell

Fig. 20 shows the segment cross-section of a cone shell under a circular ring load applied at its upper end [47]. The lower end of the shell is fixed. Two axisymmetric shell elements were used in our analysis. The material is steel which its modulus of elasticity and Poisson's ratio are 2.06×10^{11} N/m^2 and 0.3, respectively. The thickness of this axisymmetric shell is 0.508 cm. The total circular ring load of 103.972 N/m was applied in ten equal increments. Fig. 21 shows the load-deflection curve of the vertical displacement at the top of the segment and Table 8 lists the number of the required iterations for convergence for different algorithms. Here, the efficiency of proposed ULF method is higher than that of the kinetic DR scheme (KDR) so that using the ULF reduces the number of iterations for convergence about 7% compared with the KDR.

Moreover, the ULF method leads to a maximum reduction of iterations of up to 17.8% and 14.4% compared to the WRP and CLF, respectively, when the lowest frequency is updated once every ten iterations in average. Fig. 22 shows that the ULF, KDR and CLF methods converge to the steady state solution at a close-to-critical damping, whereas all the other methods suffer from over damping.

Please cite this article in press as: Rezaiee-pajand M et al. A new method of fictitious viscous damping determination for the dynamic relaxation method. Comput Struct (2011), doi:10.1016/j.compstruc.2011.02.002

Table 8
The number of iterations for convergence in analyzing the cone shell.

Method	Number of iterations for each load increment										Total	Improvement (%)	
	1	2	3	4	5	6	7	8	9	10		$\frac{WRP-ULF}{WRP}$	$\frac{CLF-ULF}{CLF}$
CDF	434	440	448	458	469	483	501	526	566	645	4970	17.8	14.4
WRP	433	440	448	457	468	482	501	526	566	645	4966		
NRP	498	497	490	484	514	457	485	520	550	668	5163		
DRP	460	470	483	497	518	536	558	533	576	686	5317		
CLF	358(1)	375(1)	388(1)	403(1)	422(1)	447(1)	480(1)	527(1)	604(1)	765(1)	4769(10)		
ULF	337(34)	347(23)	356(38)	368(36)	378(30)	396(34)	420(46)	445(43)	480(59)	554(75)	4081(418)		
KDR	506	409	413	374	443	418	351	414	508	543	4379		

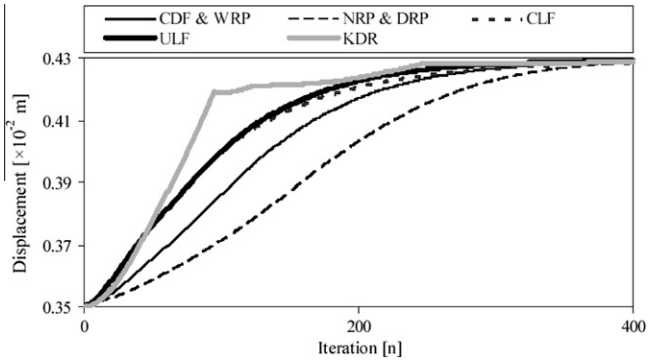

Fig. 22. Variation of the tip displacement of the cone shell during the 10th load increment.

6. Conclusion

This paper has developed a new method for determining the viscous fictitious damping for the dynamic relaxation method using the Stodola iterative process together with an instant adaptive Criterion (38). A wide range of numerical examples have shown that our new technique, either the constant lowest frequency method (CLF) or the updated lowest frequency method (ULF), can reduce the number of DR iterations significantly by guaranteeing that the convergence happens always at a closer-to-critical damping without imposing any additional calculations. Moreover, comparison of the proposed algorithms with the kinetic DR method shows that the new viscous damping can improve the basic defect of the viscous DR procedures which is their low convergence rates. In some examples, the ULF and CLF methods (proposed formulation) have higher convergence rates compared with the kinetic DR algorithm (KDR).

Appendix A

To select the suitable and compatible region for the eigenvalues of matrix $[M]^{-1}[S]$, let us investigate the variation of the error factor vs. eigenvalue. As can be seen from Fig. 1b, when an eigenvalue is close to zero, the error factor increases. It reaches unity when $\lambda = 0$. Therefore, the eigenvalues of matrix $[M]^{-1}$ should be greater than zero. Hence, Eq. (19), which presents the lower bound of each eigenvalue, can be written as:

$$\frac{Z}{(t^n)^2} \leqslant \lambda_i^L \leqslant \frac{2}{(t^n)^2} \qquad i = 1, 2, \ldots, q, \tag{A-1}$$

where, Z is a real parameter. Now, the boundaries of Eq. (A-1) are used in Regions I (Eq. (23)) and II (Eq. (24)):

$$\lambda_i \in \mathrm{I} \Rightarrow \quad \frac{Z}{(t^n)^2} \leqslant \lambda_i^L \leqslant \frac{2}{(t^n)^2} \to \frac{(t^n)^2}{Z} s_{ii} \leqslant m_{ii} \leqslant \frac{(t^n)^2}{2} \sum_{j=1}^{q} |s_{ij}| \qquad i = 1, 2, \ldots, q, \tag{A-2}$$

$$\lambda_i \in \mathrm{II} \Rightarrow \quad \frac{Z}{(t^n)^2} \leqslant \lambda_i^L \leqslant \frac{2}{(t^n)^2} \to \frac{(t^n)^2}{2} s_{ii} \leqslant m_{ii} \leqslant \frac{(t^n)^2}{Z} \left[s_{ii} - \sum_{\substack{j=1 \\ j \neq i}}^{q} |s_{ij}| \right] \qquad i = 1, 2, \ldots, q. \tag{A-3}$$

In each region, there is an acceptable domain for the fictitious mass if the stiffness elements of structure satisfy the following conditions:

$$s_{ii} \leqslant \frac{Z}{2 - Z} \sum_{\substack{j=1 \\ j \neq i}}^{q} |s_{ij}| \quad i = 1, 2, \ldots, q, \qquad \lambda_i \in I \tag{A-4}$$

$$s_{ii} \geqslant \frac{2}{2 - Z} \sum_{\substack{j=1 \\ j \neq i}}^{q} |s_{ij}| \quad i = 1, 2, \ldots, q. \qquad \lambda_i \in II \tag{A-5}$$

Parameter Z varies between 0 and 2 and, therefore, the coefficients of Eqs. (A-4) and (A-5) lead to the following boundaries:

$$0 < Z < 2 \Rightarrow 0 < \frac{Z}{2 - Z} < \infty, \qquad \lambda_i \in \mathrm{I} \tag{A-6}$$

$$0 < Z < 2 \Rightarrow 1 < \frac{2}{2 - Z} < \infty. \qquad \lambda_i \in \mathrm{II} \tag{A-7}$$

From Eq. (A-7), it is clear that the coefficient of Eq. (A-5) is always greater than unity. On the other hand, in each row of the linear structural stiffness matrix, the diagonal component is greater than or equal to the absolute value of the summation along the rest of the row:

$$s_{ii} \geqslant \sum_{\substack{j=1 \\ j \neq i}}^{q} |s_{ij}| \qquad i = 1, 2, \ldots, q. \tag{A-8}$$

Consequently, Eq. (A-5) is not valid for all real structures, because coefficient $(\frac{2}{2-Z})$ is always greater than unity. In other words, there are structures whose elements of stiffness matrix may not satisfy Eq. (A-5). Therefore, Region II is not proper for the structural analysis, while Region I is.

References

[1] Felippa CA, *Nonlinear finite element methods*, ASEN 5017, course material, http://kaswww.colorado.edu/courses.d/NFEMD/; Spring 1999.
[2] Otter JRH. Dynamic relaxation. Proc Instn Civ Engrs 1966;35:633–56.
[3] Day AS. An introduction to dynamic relaxation. The Engineer 1965;219:218–21.
[4] Frankel SP. Convergence rates of iterative treatments of partial differential equations. Mathl Tabl Natn Res Coun 1950;4:65–75.
[5] Welsh AK. Discussion on dynamic relaxation. Proc Instn Civ Engrs 1967;37:723–50.
[6] Cassell AC, Kinsey PJ, Sefton DJ, Wood WL. Cylindrical shell analysis by dynamic relaxation. Proc Instn Civ Engrs 1968;39:75–84.

Please cite this article in press as: Rezaiee-pajand M et al. A new method of fictitious viscous damping determination for the dynamic relaxation method. Comput Struct (2011), doi:10.1016/j.compstruc.2011.02.002

[7] Rushton KR. Large deflection of variable-thickness plates. Int J Mech Sci 1968;10:723–35.
[8] Brew JS, Brotton M. Non-linear structural analysis by dynamic relaxation method. Int J Numer Methods Eng 1971;3:463–83.
[9] Wood WL. Note on dynamic relaxation. Int J Numer Methods Eng 1971;3:145–7.
[10] Bunce JW. A note on estimation of critical damping in dynamic relaxation. Int J Numer Methods Eng 1972;4:301–4.
[11] Alwar RS, Rao NR, Rao MS. Altenative procedure in dynamic relaxation. Comput Struct 1975;5:271–4.
[12] Cassell AC, Hobbs RE. Numerical stability of dynamic relaxation analysis of non-linear structures. Int J Numer Methods Eng 1976;10:1407–10.
[13] Cundall PA, Explicit finite-difference methods in geomechanics. *Proceeding 2nd International Conference on Numerical Methods in Geomechanics.* Blacksburg, Virginia, June, 1976;1:132–50.
[14] Frieze PA, Hobbs RE, Dowling PJ. Application of dynamic relaxation to the large deflection elasto-plastic analysis of plates. Comput Struct 1978;8: 301–310.
[15] Papadrakakis M. A method for automatic evaluation of the dynamic relaxation parameters. Comput Methods Appl Mech Eng 1981;25:35–48.
[16] Underwood P. Dynamic relaxation. In: Belytschko T, Hughes TJR, editors. Computational method for transient analysis. Computational methods in mechanics, vol. 1. Elsevier Science; 1983. p. 245–56. Chapter 5.
[17] Felippa CA. Dynamic relaxation under general increment control. Math Prog 1982;24:103–33.
[18] Zienkiewicz OC, Lohner R. Accelerated relaxation or direct solution future prospects for FEM. Int J Numer Methods Eng 1985;21:1–11.
[19] Barnes MR. Form finding and analysis of prestressed nets and membranes. Comput Struct 1988;30(3):685–95.
[20] Shawi FAN, Mardirosion AH. An improved dynamic relaxation method for the analysis of plate bending problems. Comput Struct 1987;27:237–40.
[21] Qiang S. An Adaptive dynamic relaxation method for non-linear problems. Comput Struct 1988;30:855–9.
[22] Zhang LC, Yu TX. Modified adaptive dynamic relaxation method and its application to elastic-plastic bending and wrinkling of circular plates. Comput Struct 1989;34:609–14.
[23] Turvey GJ, Salehi M. DR large deflection analysis of sector plates. Comput Struct 1990;34:101–12.
[24] Bardet JP, Proubet J. Adaptive dynamic relaxation for statics of granular materials. Comput Struct 1991;39:221–9.
[25] Ramesh G, Krishnamoorthy CS. Post-buckling analysis of structures by dynamic relaxation. Int J Numer Methods Eng 1993;36:1339–64.
[26] Ramesh G, Krishnamoorthy CS. Inelastic post-buckling analysis of truss structures by Dynamic Relaxation method. Int J Numer Methods Eng 1994;37:3633–57.
[27] Zhang LC, Kadkhodayan M, Mai YW. Development of the maDR method. Comput Struct 1994;52:1–8.
[28] Kadkhodayan M, Zhang LC. A consistent DXDR method for elastic-plastic problems. Int J Numer Methods Eng 1995;38:2413–31.
[29] Kadkhodayan M, Zhang LC, Swerby R. Analysis of wrinkling and buckling of elastic plates by DXDR method. Comput Struct 1997;65:561–74.
[30] Topping BHV, Khan AI. Parallel schemes for dynamic relaxation, engineering computations. Int J Comput Aided Eng Software 1994;11:513–48.
[31] Ivanyi P, Topping BHV. Parallel dynamic relaxation form-finding. In: Papadrakakis M, Topping BHV, editors. Innovative Comput Meth Struct Mech. Edinburgh: Saxe-Coburg Publications; 1999. p. 127–47. Chapter 7.
[32] Pasqualino IP, Estefan SF. A nonlinear analysis of the buckle propagation problem in deepwater piplines. Int J Solids Struct 2001;38:8481–502.
[33] Wood RD. A simple technique for controlling element distortion in dynamic relaxation form-finding of tension membranes. Comput Struct 2002;80:2115–20.
[34] Han SE, Lee KS. A study on stabilizing process of unstable structures by Dynamic Relaxation method. Comput. Struct. 2003;80:1677–88.
[35] Adriaenssens SML, Barnes MR. Tensegrity spline beam and grid shell structures. Eng Struct 2001;23:29–36.
[36] Dezso Hegyi, Istvan Sajtos, Gyorgy Geiszter, Krisztian Hincz. Eight-node quadrilateral double-curved surface element for membrane analysis. Comput Struct 2006;84:2151–8.
[37] Domer B, Fest E, Lalit V, Smith IFC. Combining dynamic relaxation method with artificial neural networks to enhance simulation of tensegrity structures. ASCE J Struct Eng 2003;129(5):672–81.
[38] Turvey GJ, Salehi M. Annular sector plates: comparison of full-section and layer yield prediction. Comput Struct 2005;83:2431–41.
[39] Topping BHV, Ivanyi P. Computer aided design of cable-membrane structures. Saxe-Coburg Publications on Computational Engineering; 2007. Chapter 3, p. 39–82.
[40] Kadkhodayan M, Alamatian J, Turvey GJ. A new fictitious time for the dynamic relaxation (DXDR) method. Int J Numer Methods Eng 2008;74:996–1018.
[41] Rezaiee-Pajand M, Alamatian J. Nonlinear dynamic analysis by dynamic relaxation method. J Struct Eng Mech 2008;28(5):549–70.
[42] Brualdi RA, Mellendorf S. Regions in the complex plane containing the eigenvalues of a matrix. Am Math Month 1994;101(10):975–85.
[43] Clough RW, Penzien J. Dynamics of structures. 2nd ed. New York: McGraw Hill; 1993.
[44] Chopra AK. Dynamics of structures; theory and applications to earthquake engineering. 2nd ed. India: Prentice Hall; 2002.
[45] Wood RD, Zienkiewicz OC. Geometrically nonlinear finite element analysis of beams, frames, arches and axisymmetric shells. Comput Struct 1977;7:725–35.
[46] Yang YB, Yang CT, Chang TP, Chang PK. Effects of member buckling and yielding on ultimate strength of space trusses. J Struct Eng ASCE 1997;19(2):179–91.
[47] Teng JG, Rotter JM. Elastic-plastic large deflection analysis of axisymmetric shells. Comput Struct 1989;31(2):211–33.

Please cite this article in press as: Rezaiee-pajand M et al. A new method of fictitious viscous damping determination for the dynamic relaxation method. Comput Struct (2011), doi:10.1016/j.compstruc.2011.02.002